to $\epsilon_j \mathrm{Tr}[\sigma^{+j}\Psi(y_1)\bar{\Psi}(y_2)]$. The expansion of the operator product contains terms proportional to the scalar gluon field $\varphi(x)$ such as

$$|\vec{y}_1-\vec{y}_2|^{(-1+\gamma_\varphi-2\gamma_\psi)}\vec{\epsilon}\cdot(\vec{y}_1-\vec{y}_2)|\vec{y}_1-\vec{y}_2|^{-1}\int_0^1 d\alpha\, a(\alpha)\partial_-(0,\vec{y}_2,\alpha y_1^- +(1-\alpha)y_2^-).$$

This quark-antiquark singularity leads to a term in $\mathcal{P}(x,\vec{k})$ that falls off as

$$\mathcal{P}_{qq}(x,\vec{k})\propto|\vec{k}|^{(-2+2\gamma_\psi-\gamma_\varphi)}\approx|\vec{k}|^{-2}.$$

Thus one obtains another $|\vec{Q}_T|^{-2}$ term in the μ-pair cross section, corresponding, for example, to the Feynman diagram in Fig. 1(b).

I thank J. Bjorken and J. Gunion for emphasizing the importance of final-state jets to me, and D. Gross and S. Treiman for helpful critical advice.

*Work supported by the National Science Foundation under Grant No. MPS-75-22514.

[1]R. P. Feynman, *Photon-Hadron Interactions* (Benjamin, Reading, Mass., 1972); J. D. Bjorken, in *Proceedings of the Third International Symposium on Electron and Photon Interactions at High Energies*, Stanford Linear Accelerator Center, Stanford, California, 1967 (Clearing House of Federal Scientific and Technical Information, Washington, D. C., 1968); J. D. Bjorken and E. A. Paschos, Phys. Rev. 185, 1975 (1969).

[2]S. D. Drell, D. Levy, and T.-M. Yan, Phys. Rev. 187, 2159 (1969), and Phys. Rev. D 1, 1935 (1970). See the related work of J. F. Gunion, S. J. Brodsky, and R. Blankenbecler, Phys. Rev. D 8, 287 (1973); S. J. Brodsky, F. E. Close, and J. F. Gunion, Phys. Rev. D 8, 3678 (1973); P. V. Landshoff, J. C. Polkinghorne, and R. Short, Nucl. Phys. B28, 225 (1971).

[3]D. Gross and F. Wilczek, Phys. Rev. Lett. 30, 1343 (1973); H. D. Politzer, Phys. Rev. Lett. 30, 1346 (1973).

[4]S. D. Drell and T.-M. Yan, Phys. Rev. Lett. 25, 316 (1970), and Ann. Phys. (N.Y.) 66, 578 (1971).

[5]G. Farrar, Nucl. Phys. B77, 429 (1974).

[6]G. Chu and J. F. Gunion, Phys. Rev. D 10, 3672 (1974); J. F. Gunion, Phys. Rev. D 14, 1400 (1976).

[7]J. B. Kogut and D. E. Soper, Phys. Rev. D 1, 2901 (1970); R. A. Neville and F. Rohrlich, Phys. Rev. D 3, 1382 (1971).

[8]J. D. Bjorken, J. B. Kogut, and D. E. Soper, Phys. Rev. D 3, 1382 (1971).

[9]D. E. Soper, to be published.

[10]That is, "null-plane helicity." See D. E. Soper, Phys. Rev. D 5, 1956 (1972).

[11]K. Wilson, Phys. Rev. 179, 1499 (1969).

[12]If one assumes conformal invariance near the light cone, one obtains such a representation with $a(\alpha)$ known. See S. Ferrara, R. Gatto, and A. F. Grillo, Nucl. Phys. B34, 349 (1971).

Improved Experimental Test of Time-Reversal Symmetry in ^{19}Ne β Decay*

R. M. Baltrusaitis and F. P. Calaprice
Joseph Henry Laboratories, Princeton University, Princeton, New Jersey 08540
(Received 15 December 1976)

We report on a new measurement of the time-reversal–violating triple angular correlation between the nuclear spin and the positron and neutrino directions $D\hat{J}\cdot(\vec{v}_\beta\times\hat{q}_\nu)$. Our result for the decay process $^{19}\mathrm{Ne}\rightarrow{}^{19}\mathrm{F}^- + e^+ + \nu$ is $D = -0.0005 \pm 0.0010$, consistent with time-reversal symmetry.

We have developed new experimental techniques for testing time-reversal invariance in ^{19}Ne beta decay which are substantially more sensitive than methods employed in earlier investigations on this system. We test T invariance by searching the spectrum for an angular correlation of the form $D\hat{J}\cdot(\vec{v}\times\hat{q})$, where $\hat{J}$ is the initial nuclear spin direction and $\vec{v}$ and $\hat{q}$ are the positron velocity and neutrino directions, respectively. The triple correlation is observed by detecting the positron and recoil F^- ion which result from the polarized nuclear decay $^{19}\mathrm{Ne}\rightarrow{}^{19}\mathrm{F}^- + e^+ + \nu$. A nonzero value of D would signal the breakdown of T invariance, provided final-state interactions are negligible. Our motivation for these studies continues to be to provide new data which may help to clarify the phenomenon of CP nonconservation in the neutral kaon system.[1]

As in the two previous tests in ^{19}Ne,[2,3] we use the atomic-beam method to achieve nuclear polarization. The noble-gas atomic-beams machine has been described previously in the literature,[2,3] and is shown schematically in Fig. 1. After state selection by means of the Stern-Gerlach magnet, the polarized atoms enter the storage cell via slit S_6, a long narrow channel that restricts the outflow of atoms and results in a mean sitting time of 1–2 sec for atoms in the cell. A pair of Helmholtz coils centered about the cell and coaxial with the beam axis produce a uniform field of 15 G to maintain the polarization. The nonuniform field of the Stern-Gerlach magnet is prevented from fringing into the cell by magnetic shielding, and two orthogonal pairs of Helmholtz coils are

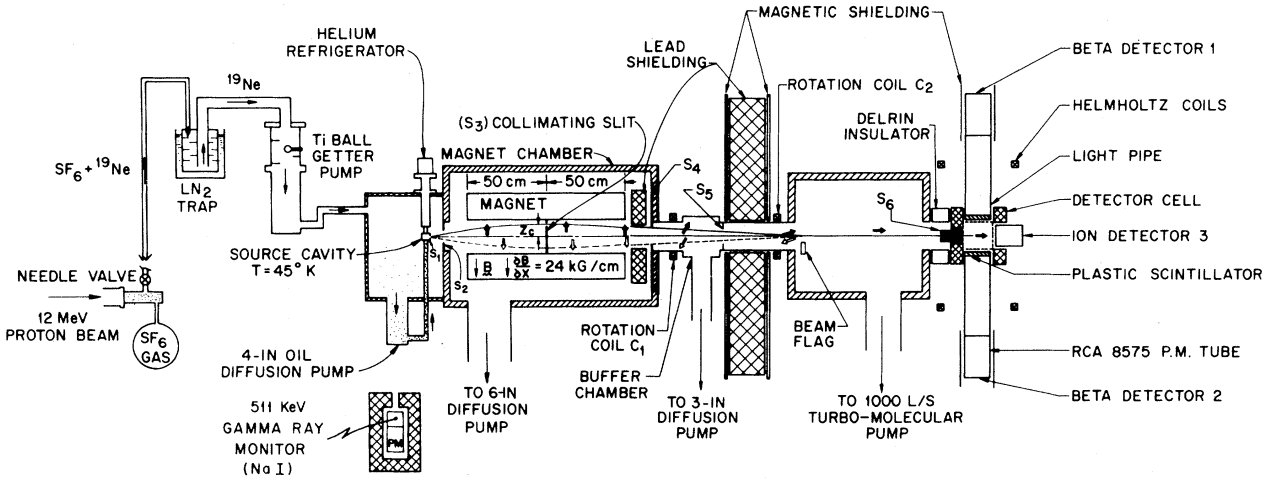

FIG. 1. Schematic diagram of the atomic-beam apparatus (not to scale). ^{19}Ne is produced by the reaction ^{19}F(p, n)^{19}Ne, using a 20-μA beam of 12-MeV protons from the Princeton University cyclotron. SF_6 gas is used as the target and as a carrier gas for the ^{19}Ne. The SF_6 is condensed in a liquid nitrogen trap, and the ^{19}Ne pumped into the source chamber where it is cooled to 45°K. The ^{19}Ne diffuses out of the source slit S_1 into the magnet chamber, where the strong field gradient (~24 kG/cm) splits the beam into the two nuclear magnetic substates, $m_j = \pm \frac{1}{2}$. Suitable positioning of slit S_3 selects one substate, with essentially 100% polarization. Coils C_1 and C_2 rotate the polarization along the beam axis. The solid line through slits S_1, S_3 and S_6 shows the path of ^{19}Ne atoms with nuclear spin "up".

used to cancel nonaxial stray fields. The field is uniform to within 0.2% over the volume of the cell and while this uniformity permits much longer sitting times without noticeable loss of polarization, we have experienced ion detector difficulties with times longer than 1–2 sec because of pressure buildup due to outgassing in the cell.

An illustration of the cell as viewed looking along the beam axis is shown in Fig. 2. The main body of the cell consists of an aluminum cube (10 cm on a side) which is hollowed out to have a cubical cavity 4 cm on a side. The polarized ^{19}Ne enters the cavity through channel S_6 which penetrates one side of the aluminum cube. Two β detectors and three ion detectors are located on the other five sides of the aluminum cube; these extend into the cube to face five sides of the cavity. The β detectors consist of 1-cm-thick Pilot B plastic scintillators coupled through Lucite light pipes to RCA 8575 photomultiplier tubes. Aluminum foil is placed directly in front of the scintillators to prevent optical cross-talk betwen the β detectors and to confine the ^{19}Ne atoms within the cavity.

The F^- ions are detected with microchannel plate electron multipliers. The two shown in Fig. 2 are 4 cm×4 cm squares which were fabricated to order by Galileo Electro-Optics Corp. Each detector has two 1-mm-thick plates in tandem to provide sufficient gain for ion event pulses to be distinguished from noise. After a ^{19}Ne decay, the F^- ion recoils freely (maximum energy 200 eV) through the electric-field-free region of the central cavity, passes through a fine gold mesh, and is then accelerated to 5 keV before impacting on the channel plate. The inset to Fig. 3 illus-

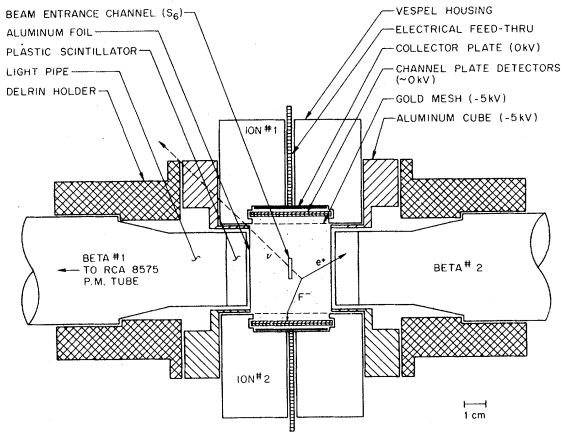

FIG. 2. Expanded scale drawing of the storage cell showing the detectors used in the measurement of the time-reversal correlation. The dots represent ^{19}Ne atoms and the decay products from a typical decay are shown. The positron is promptly detected with a plastic scintillator; the recoil ion drifts freely through the inner zero-electric-field region and is then accelerated to 4 keV and detected by a channel plate electron multiplier.

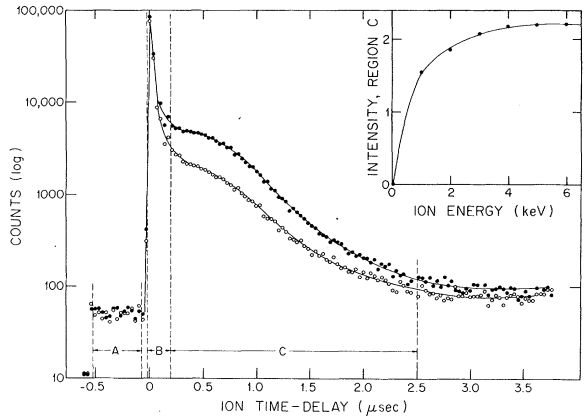

FIG. 3. The time-delay spectra for ions detected in ion detector 3. The two spectra, taken with opposite polarizations, illustrate the large neutrino-spin correlation $B\hat{J}\cdot\hat{q}_\nu$. Events in region A are accidental coincidences, region B prompt coincidences, and region C delayed coincidences due to ions originating in the field-free part of the cell.

trates the efficiency of the channel plate as a function of the ion energy. At 5 keV the efficiency of the detector is at a maximum; the transmission of the gold mesh and the active area of the channel plate, however, limit the overall efficiency of the detector to 50%. The ^{19}Ne is uniformly dispersed throughout the cavity including the volume containing the ion detectors (see dots on Fig. 2).

To measure the time-reversal correlation we use the β-ion detector pairs illustrated in Fig. 2. With the polarization along the beam axis, the asymmetry of delayed coincidence events between the pairs $\beta_1 I_1$ and $\beta_1 I_2$ is proportional to D and similarly for $\beta_2 I_1$ and $\beta_2 I_2$. As a test of the overall sensitivity of the system, we employ a third ion detector which is located along the polarization axis (see Fig. 1, ion detector 3). The delayed coincidence rate into this detector is sensitive to the large neutrino asymmetry, $BP\hat{J}\cdot\hat{q}_\nu$ where $B\approx -1$ for ^{19}Ne decay and P is the actual polarization in the cell. In this way we measure a known quantity which is sensitive to the polarization and general conditions within the cell at the same time as we measure the time-reversal correlation.

The data are accumulated as follows. Delayed coincidence events in which either positron signal is followed within 4 μsec by any of the three ion-detector pulses are accepted as "coincidence events" and stored in an on-line computer. For each of these events we record five parameters on magnetic tape: The energy signal for each positron detector and the ion time-delay signal from each of three separate time-to-amplitude converters. Each time-to-amplitude converter is started by either positron detector and stopped by one of the three ion detectors. For a normal event there are just two nonzero parameters—one β energy and one time delay—and thus the five parameters uniquely determine the detector pair. In addition to the normal events, about 15% of the coincidences are events with more than one β or more than one ion signal; these are due to β backscatters, β-γ (511 keV) coincidences, or ion-detector cross-talk, and while these events are recorded, they are not used for the determination of the angular correlations. The singles events are counted external to the computer. Finally, data are taken in both polarization states by reversing S_3 every 15 min; the polarization is also reversed by reversing the direction of the axial holding field —in this case, to cancel a spurious effect associated with field misalignment.

Figure 3 illustrates the time-delay spectra of ion detector 3 in coincidence with either positron detector. The two spectra were taken with opposite polarization directions and are normalized to correspond to the same number of disintegrations within the cell. All β energies from 0.6 to 2.2 MeV are accepted. The stop signal from the ion detector is delayed by 0.5 μsec to offset the zero-time-delay point and allow a measurement of the accidental coincidences (region A). The sharp prompt peak (region B) is due to detection in the channel plate of electrons or x-rays from atomic shake-off processes, as well as from ions originating from decay sites between the mesh and the channel plate. Region C has events due to true F^- recoil ions that originate in the field-free part of the cell, as well as accidental coincidences which amount to 4% of the trues in this region.

The large difference in the spectra for the two polarizations in region C of Fig. 3 is due to the neutrino-spin angular correlation $B\hat{J}\cdot\hat{q}$. Thus, the number of counts in region C of each spectrum is proportional to $1\pm\Delta_B$, where $\Delta_B = G_B S_e S_I P B$; P is the magnitude of the polarization, S_e and S_I are factors that allow for positron and ion backscattering, and G_B is a geometry correction which accounts for the average of $\hat{J}\cdot\hat{q}$ over all observed $\beta_{1,2}I_3$ events. For the β energy range 0.6–2.2 MeV and time-delay interval 0.2–2.5 μsec, Monte Carlo calculations yield $G_B = 0.40\pm0.01$. The measured asymmetry for one run is $\Delta_B{}^{\exp} = -0.347\pm0.002$. Combining this with the value

$B = -0.998$ (Ref. 3) we compute $PS_eS_I = 0.86 \pm 0.02$. This result indicates that there is a 14% washout of the asymmetry beyond the washout allowed by the geometry factor. Independent studies of the polarization (made using the β asymmetry) indicate that the polarization is essentially 100% and thus the 14% washout appears to be caused by a combination of electron and ion backscattering.

To determine the time-reversal correlation parameter we first note that the $\beta_1 I_1$ and $\beta_1 I_2$ coincidence counts may be expressed as follows:

$$N_{\beta_1 I_1}{}^{\pm} = k^{\pm} \epsilon_{\beta_1}{}^{\pm} \epsilon_{I_1}{}^{\pm} (1 \mp \Delta_D{}^{\pm}), \quad (1)$$

$$N_{\beta_1 I_2}{}^{\pm} = k^{\pm} \epsilon_{\beta_1}{}^{\pm} \epsilon_{I_2}{}^{\pm} (1 \pm \Delta_D{}^{\pm}). \quad (2)$$

Here the ($\pm$) signs refer to the two polarization states, k is the number of disintegrations in the cell, ϵ is the detector efficiency, and $\Delta_D = G_D S_e S_I \times P\langle v/c\rangle D$. Similar relations hold for the $\beta_2 I_1$ and $\beta_2 I_2$ coincidences and the counts can therefore be combined to yield the following:

$$(R)_{+\hat{z}} = \frac{N_{\beta_1 I_1}{}^{+} N_{\beta_1 I_2}{}^{-} N_{\beta_2 I_1}{}^{-} N_{\beta_2 I_2}{}^{+}}{N_{\beta_1 I_1}{}^{-} N_{\beta_1 I_2}{}^{+} N_{\beta_2 I_1}{}^{+} N_{\beta_2 I_2}{}^{-}} = \left(\frac{1-\Delta_D}{1+\Delta_D}\right)^4. \quad (3)$$

The subscript on R refers to the fact that all these data correspond to having the axial field parallel to the beam (z) axis. A similar relationship is obtained for the field antiparallel to the beam axis. Thus the final combination of all data which is used to determine Δ_D is

$$R_{\text{tot}} = (R)_{+\hat{z}} (R)_{-\hat{z}} = \left(\frac{1-\Delta_D}{1+\Delta_D}\right)^8. \quad (4)$$

The value of Δ_D obtained from all data for the energy and time delay intervals 0.6–2.2 MeV and 0.2–2.5 μsec, respectively, is $\Delta_D{}^{\text{exp}} = -0.000\,14 \pm 0.000\,26$. By Monte Carlo calculation, the corresponding geometry and v/c factors are found to give $G_D\langle v/c\rangle = 0.30 \pm 0.01$. We now assume that the backscatter correction factors S_e and S_I are the same here as for the neutrino-asymmetry case and rely on the measurement of Δ_B to specify the combination $PS_eS_I = 0.86$, as given above. With the correction factors and Δ_D as given, the time-reversal correlation parameter is computed to be

$$D_{\text{exp}} = -0.0005 \pm 0.0010, \quad (5)$$

where the uncertainty is purely statistical.

The above result for D is consistent with time-reversal invariance. In the allowed approximation D is related to the Fermi and Gamow-Teller form factors, $a = C_V M_F$ and $c = C_A M_{GT}$, respectively, by the expression[4]

$$D = \frac{2}{\sqrt{3}} \frac{\text{Im} a^* c}{a^2 + c^2}. \quad (6)$$

Regarding the nuclear matrix elements M_F and M_{GT} as relatively real and with $a = 1$ and $c \cong -1.6$, we obtain a limit on the phase angle between the vector and axial-vector coupling constants given by

$$\varphi_{VA} = 179.94 \pm 0.11°. \quad (7)$$

This represents a factor of 4 improvement over the previous ^{19}Ne experiment and is a factor of 2 better than the limit placed by the most precise measurement of D for the neutron decay.[5]

The precision of the present experiment is almost at the level of the expected final-state electromagnetic contribution to D. This effect is present even in the absence of a violation of time-reversal invariance; and it has been shown that the main contribution arises from the weak magnetism[6] and induced tensor[7] form factors. Allowing for just the weak magnetism form factor, as given by conserved vector current,[8] and averaging the expression for D^{EM} given in Ref. (7) over the β energy range 0.6–2.2 MeV, we compute $D^{EM} \approx +1.6 \times 10^{-4}$. This is increased to $+4 \times 10^{-4}$ if a tensor form factor of the size indicated by recent measurements on the ^{19}Ne decay[8] is also included. Thus, by a modest improvement of our present result, $D = (-5 \pm 10) \times 10^{-4}$, we should be able to detect the final-state terms; these are interesting with respect to the second-class-current problem,[8] quite apart from the question of T symmetry. We are investigating the possibility of reducing the error to $(1-2) \times 10^{-4}$ by improving the cell vacuum so as to permit longer sitting times and therefore higher count rates.

We wish to thank Professor E. D. Commins, Professor B. R. Holstein, and Professor S. B. Treiman for useful discussions. Special thanks are also due to Mr. L. Varga whose expert craftsmanship was essential in fabricating the cell.

*Work supported in part by the National Science Foundation.

[1]C. R. Christenson, J. W. Cronin, V. L. Fitch, and R. Turlay, Phys. Rev. Lett. 13, 138 (1964).

[2]F. P. Calaprice, E. D. Commins, H. M. Gibbs, G. L. Wick, and D. A. Dobson, Phys. Rev. 184, 1117 (1969).

[3]F. P. Calaprice, E. D. Commins, and D. C. Girvin, Phys. Rev. D 9, 519 (1974).

[4]J. D. Jackson, S. B. Treiman, and H. W. Wyld, Jr., Phys. Rev. 106, 517 (1957). See also B. R. Holstein,

Phys. Rev. C 5, 1529 (1972).
[5]R. I. Steinberg, P. Liaud, B. Vignon, and V. W. Hughes, Phys. Rev. Lett. 33, 41 (1974).
[6]C. G. Callan and S. B. Treiman, Phys. Rev. 162, 1494 (1967).
[7]See Holstein, Ref. 4.
[8]F. P. Calaprice, S. J. Freedman, W. C. Mead, and H. C. Vantine, Phys. Rev. Lett. 35, 1566 (1975).

Observation of an Anomalous Structure in Proton Polarization from Deuteron Photodisintegration

T. Kamae, I. Arai, T. Fujii, H. Ikeda, N. Kajiura, S. Kawabata, K. Nakamura,* K. Ogawa, and H. Takeda
Department of Physics, University of Tokyo, Bunkyo-ku, Tokyo, Japan 113

and

Y. Watase
National Laboratory for High Energy Physics, Tsukuba-gun, Ibaraki, Japan 300-32
(Received 31 August 1976)

Proton polarization in $\gamma d \to pn$ has been measured at c.m. angle around 90° and photon energies from 325 to 725 MeV. The polarization increases sharply with the photon energy, reaching a high maximum of $(-80 \pm 8)\%$ around 500–550 MeV. Such a high polarization with a sharp energy dependence seems to indicate a new effect in the dibaryon system.

Photodisintegration of the deuteron offers one of the simplest ways for studying a highly excited dibaryon system. Previous measurements have shown that the total cross section has a peak around 300 MeV and decreases monotonically with energy up to 800 MeV.[1,2] These gross features are consistent with the assumption that main contributions come from the Born term and the nucleon-resonance term as shown in Fig. 1.

However, further studies of the differential cross section, the recoil proton polarization, and the polarized photon asymmetry have also revealed the shortcomings of theoretical analyses based on these terms.[3,4] In particular, the analyses failed to explain a sharp increase of proton polarization observed in the energy range of 300 to 450 MeV.[5,6] Since the recoil proton polarization is sensitive to the existence of imaginary interfering amplitudes, the extention of polarization measurements to higher energy ranges is a vital step towards better understanding of this process.

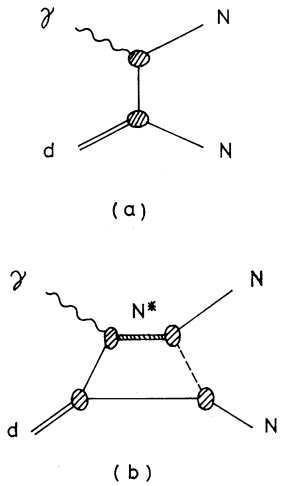

FIG. 1. Dominant diagrams for $\gamma d \to pn$ in the present energy range: (a) nucleon Born term; (b) NN^* term.

The experimental layout is shown in Fig. 2. Bremsstrahlung photons produced by electrons accelerated in the synchrotron at the Institute for Nuclear Study, University of Tokyo, were brought to a liquid deuterium target. A magnetic spec-

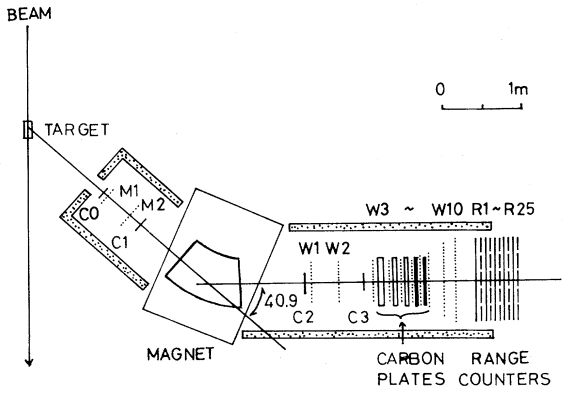

FIG. 2. Experimental layout.